Appl Phys A (2009) 95: 781–787
DOI 10.1007/s00339-009-5071-z

Applied Physics A
Materials Science & Processing

Simple fabrication of hexagonally well-ordered AAO template on silicon substrate in two dimensions

Nevin Taşaltın · Sadullah Öztürk · Necmettin Kılınç ·
Hayrettin Yüzer · Zafer Ziya Öztürk

Received: 4 April 2008 / Accepted: 15 December 2008 / Published online: 20 January 2009

Abstract In this study, thin anodic aluminum oxide (AAO) templates both on silicon substrates (AAO template/SiO_2/Si) and Ti-coated silicon substrates (AAO template/Ti/SiO_2/Si) were developed for design of magnetic, electronic and optoelectronic devices, chemical sensors and chip-scale lithium-ion rechargeable microbatteries. Two types of AAO template were prepared by using a two-step anodization procedure. The templates were characterized by scanning electron microscopy and energy dispersive X-ray spectroscopy. The obtained thin AAO templates were approximately 50 nm in diameter and 700 nm in length with 80-nm interpore distances in a relatively large area of 6 cm^2. A barrier layer of the AAO templates was removed by a cathodic polarization method in KCl solution for several seconds. The current–time transient during removing the alumina barrier layer of the thin AAO template and the mechanism of electrochemical dissolution of the barrier layer are given in detail.

N. Taşaltın · S. Öztürk · N. Kılınç · Z.Z. Öztürk
Department of Physics, Gebze Institute of Technology,
41400 Gebze Kocaeli, Turkey

N. Taşaltın
e-mail: ntasaltin@gyte.edu.tr

S. Öztürk
e-mail: sadullahozturk@gyte.edu.tr

N. Kılınç
e-mail: nkilinc@gyte.edu.tr

Z.Z. Öztürk (✉) · H. Yüzer
TUBITAK Marmara Research Centre, P.O. Box 21, 41470 Gebze
Kocaeli, Turkey
e-mail: zozturk@gyte.edu.tr
Fax: +90-262-6538490

H. Yüzer
e-mail: Hayrettin.Yuzer@mam.gov.tr

PACS 81.07.De · 81.16.Be · 82.45.Yz

1 Introduction

In recent years, a self-assembly anodic aluminum oxide (AAO) template is one of the most prominent materials that has attracted much interest for fundamental scientific research and provided to miniaturize magnetic, electronic and optoelectronic devices and chemical sensors due to the high aspect ratio, high pore density, high level of ordering and uniformity [1]. Many studies have demonstrated that AAO is an excellent template or mask material for the fabrication of one-dimensional nanostructures [2, 3] and two-dimensional patterns [4, 5] as well as in the design of various AAO-based nanodevices. Besides, an AAO template is used for power sources such as a chip-scale lithium-ion rechargeable microbattery having high power and capacity. Nowadays, a lithium-ion rechargeable microbattery can be realized by fabricating nanowire-based cathodes directly on Si substrates. These nanowire cathodes provide greater surface area, thus enhancing power [6].

The first papers in the field are Masuda and Fukuda in 1995 [7] and Jessensky et al. in 1998 [8]. These papers describe how to fabricate an AAO template on Al foil with ordered hexagonally parallel nanotubes using a twostep anodization technique. The nanotubes are becoming ordered from the bottom up in the anodization process. To have them completely ordered all through the template it is necessary to introduce a pre-arranged pattern before anodization. They suggested that the anodization should be carried out in two steps. By controlling the voltage during anodization, it is possible to control the interpore distance as well as the pore diameters. The thickness of the template can be tailored by controlling the time for the second anodization.

Several previous studies revealed that a self-ordered AAO template can only be obtained under specific conditions. For example, structures with pore spacings of 50, 65, 100, 420 and 500 nm are fabricated at 19 and 25 V in sulfuric acid, at 40 V in oxalic acid and at 160 and 195 V in phosphoric acid, respectively [7–9]. Besides, Gösele and coworkers [10–13] reported a new anodization process for an AAO template on Al foil. This process was a new generation of the so-called 'hard anodization' approach that has been widely used in industry for high-speed fabrication of mechanically robust, very thick and low-porosity alumina films. The pore-formation mechanism for fabrication of an AAO template is given schematically in regime 4 in Fig. 1 [9].

At the beginning of the anodization, an aluminum oxide barrier layer, which consists of non-conductive oxide, covers the entire surface of the aluminum. The electric field is focused locally on fluctuations of the surface. This leads to field-enhanced and/or temperature-enhanced dissolution in the formed aluminum oxide and thus to the growth of pores. Since some pores begin to stop growing due to competition among the pores, the current decreases again. Finally, pores grow in a stable manner [9].

However, there is a main problem that is encountered in the fabrication of an AAO template. It is well known that there is a hemispherical alumina barrier layer existing between the bottom of the nanotubes and the substrate in applications such as dc electrodeposition of metal nanowires. Typically, this insulating barrier layer has a thickness of 2–100 nm [14]. It can block the direct electrical contact between the nanotubes and the conductive substrate.

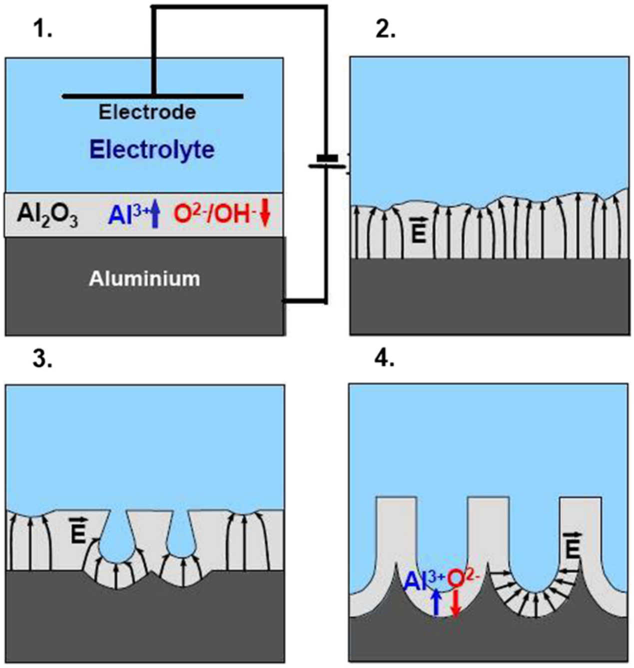

Fig. 1 Schematic diagram of the pore-formation mechanism for fabrication of AAO template. Regime 1: formation of barrier oxide on the entire area; regime 2: local field distributions caused by surface fluctuations; regime 3: creation of pores by field-enhanced or/and temperature-enhanced dissolution; regime 4: stable pore growth [9]

In a common practice to overcome these problems, the barrier layer is removed by the chemical etching of the AAO template in 5 wt.% H_3PO_4. This method has two main disadvantages. One of them is that it is difficult to handle the very thin and brittle AAO template. The other one is that this process induces isotropic chemical etching of the alumina film; they both inevitably widen the size of the AAO nanotubes. With the progressive miniaturization of electronic devices, there is now a need to study the electrical and structural properties in systems of thin nanowires (especially for chemical sensors to obtain nanowires in high surface area). A high surface area AAO template with size of the AAO nanotubes as small as a few nanometers could play an important role if an approach to remove the barrier layer without widening the original nanotube size can be developed. However, this process leaves an unsupported AAO template that is unsuitable for device design. It is therefore of great interest to develop methods to fabricate a thin AAO template on a Si substrate for device design by depositing nanowires or nanotubes directly onto the substrate. For this purpose, the aluminum oxide barrier layer of the AAO template must be removed. Electrodeposition of a metal in an AAO template on a Si wafer without removing the barrier layer has been reported, where the deposition of nanowires was achieved by using an ac method or by utilizing the tiny conduction paths that may be embedded in the alumina barrier layer. In that case, the higher barrier resistance greatly adds to the impedance of nanodevices and thus restricts their applications, such as chemical sensors. Alternatively, some methods such as the voltage drop or the constant current anodization were applied to AAO templates [15–18]. These techniques can only thin or selectively remove the barrier layer, but they cannot remove it completely. Currently, Rabin et al. [19] fabricated a 12-µm-thick AAO template on a Ti-coated Si substrate. The barrier layer was electrochemically etched away by applying cathodic bias to the AAO template in a dilute KCl aqueous solution for 15–30 min. Then, Tian et al. [20] proposed the in situ removing of the barrier layer by reversing the polarity of the voltage in the KCl solution after anodization of the Al foil. However, few detailed studies have been done about the removing of the AAO barrier layer by cathodic polarization; therefore, there is a lack of knowledge concerning the mechanism of electrochemical dissolution of the barrier layer and this drives us to investigate alternative approaches to solve the problem of removing the barrier layer.

In this study, we fabricated both AAO template/SiO_2/Si and AAO template/Ti/SiO_2/Si more simply and faster. Advantages of our study over the past studies are that we investigate the cathodic polarization method in KCl solution for

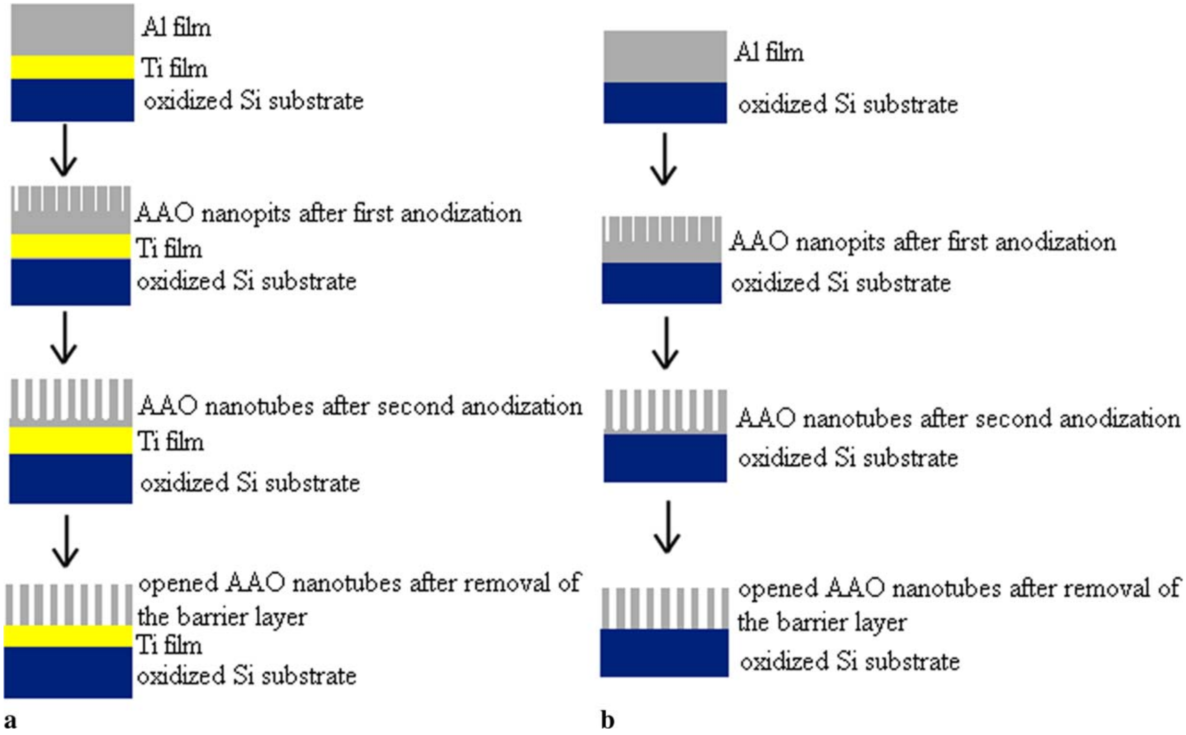

Fig. 2 Schematic diagram for describing the fabrication of well-ordered **a** AAO template/Ti/SiO_2/Si and **b** AAO template/SiO_2/Si

removing the barrier layer of a thin (700 nm) AAO template and give more details about the electrochemical dissolution mechanism of the barrier layer for the thin AAO template.

2 Experimental procedure

Two types of AAO template were prepared by using a two-step anodization procedure. The first type AAO template (AAO template/SiO_2/Si) was fabricated using the direct anodization of an Al film deposited on an n-type (100)-oriented oxidized Si substrate and the second type AAO template (AAO template/Ti/SiO_2/Si) was fabricated by anodizing an Al film deposited on a Ti/SiO_2/Si substrate. First, a 200-nm-thick Ti film was deposited on a thermally oxidized Si wafer by thermal evaporation in a vacuum chamber. The Al thin film was subsequently thermally evaporated on the Ti film with a thickness of 700 nm. The anodization was performed in a 0.3 M oxalic acid ($H_2C_2O_4$) solution at 40 V and 15°C for 20 min. Then, the anodically grown aluminum oxide films were selectively removed by dipping the samples into 5 wt.% phosphoric acid (H_3PO_4) solution at 30°C for 20 min. The second anodization was performed under the same conditions as the first. Thus, we obtained AAO template/SiO_2/Si and AAO template/Ti/SiO_2/Si. At the end of the second anodization process, the alumina barrier layer, which is the bottom of the AAO template, was removed by a cathodic polarization method. Cathodic polarization was performed in 0.2 M KCl solution by applying– 2 V to the anode for 100 s. This process is necessary to provide electrochemical deposition of metal nanowires into the AAO nanotubes for future studies. A schematic diagram for describing the fabrication of well-ordered AAO template/Ti/SiO_2/Si and AAO template/SiO_2/Si is given in Fig. 2.

3 Results and discussion

An anodic aluminum oxide film was grown by two-step anodization in oxalic acid solution at 40 V. The current density–time transient during first and second anodizations of AAO template/Ti/SiO_2/Si is given in Fig. 3. The anodic reaction is given in (1) and (2):

$$6OH^- - 6e^- \rightarrow 3H_2O + 3O^{2-}, \quad (1)$$

$$2Al + 3O^{2-} \rightarrow Al_2O_3 \text{ (amorph.)}. \quad (2)$$

The cathodic reaction is as follows:

$$6H^+ + 6e^- \rightarrow 3H_2 \text{ (gas)}. \quad (3)$$

The current behaviors arise from the formation of the barrier layer, initiation of nanotube formation and growth of the

AAO film, for the first and second anodizations showed differences. At the beginning of the oxide formation, both transients had an identical behavior. During the first anodization process, the barrier-type AAO film was grown; the current density decayed in a few seconds. After the initial 2 min, while porous-type aluminum oxide film growth was beginning, the following current density decayed exponentially and there was an obvious color change to transparent AAO after the first 2 min. Then, the current decreased as the remaining Al was completely anodized. The current increased at the end of the Al anodization. The rate of increase in current depended strongly on the uniformity of the Al film. The Al was very smooth with few defects; there was a very slow and slight increase in current and the surface of the Al film was uniform [21].

For the second anodization, the time for reaching the lowest and constant current was significantly shorter than for the first anodization. The minimum current density was higher for the second anodization than for the first anodization. The time for AAO nucleation and AAO film growth for the first anodization was longer than in the second anodization. After first anodization and selectively etching the initial AAO film, the surface was patterned with nanopits. The patterned surface remained at the bottom of each curvature, where the resistance was the lowest and the electric field was the highest; thus, the AAO nucleation was easier on a patterned surface. In addition, the thermal effects, high electric field and the change of the diffusion mechanism from planar diffusion to spherical diffusion accelerated the diffusion rate of protons to the oxide/solution interface, which resulted in great acceleration of both the AAO barrier layer dissolution and the growth of tubes. Therefore, the time for reaching a steady state was shortened. Under a constant potential, high current density in the second anodization caused the large patterned surface area.

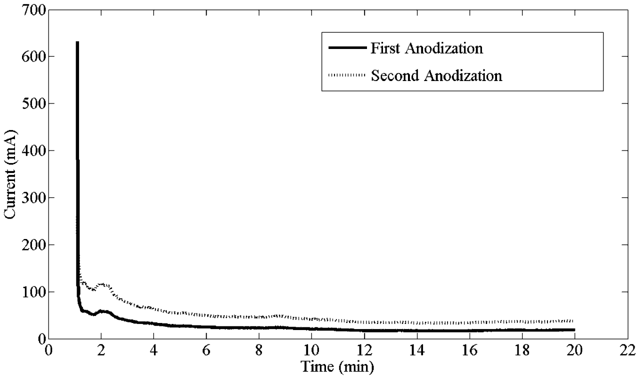

Fig. 3 Current density–time transient during first and second anodizations of the AAO template/Ti/SiO_2/Si

The morphologies of the fabricated AAO templates were characterized by scanning electron microscopy (SEM). Figure 4 shows typical top views of the AAO template after first and second anodizations. Figure 5 shows a typical top view and a cross-sectional view of the AAO template/SiO_2/Si after second anodization.

As shown in both Figs. 4 and 5, fabricated hexagonal straight nanotubes of the AAO templates were observed approximately 50 nm in diameter and 700 nm in length with 80-nm interpore distances. The initial pore arrangement was irregular on the aluminum oxide surface, but repulsive forces between neighboring pores during the anodization gave rise to self-assembly ordering. Thus, hexagonally well-ordered AAO templates were obtained. Nanopits were observed approximately 28 nm in diameter on the aluminum oxide surface after first anodization as shown in

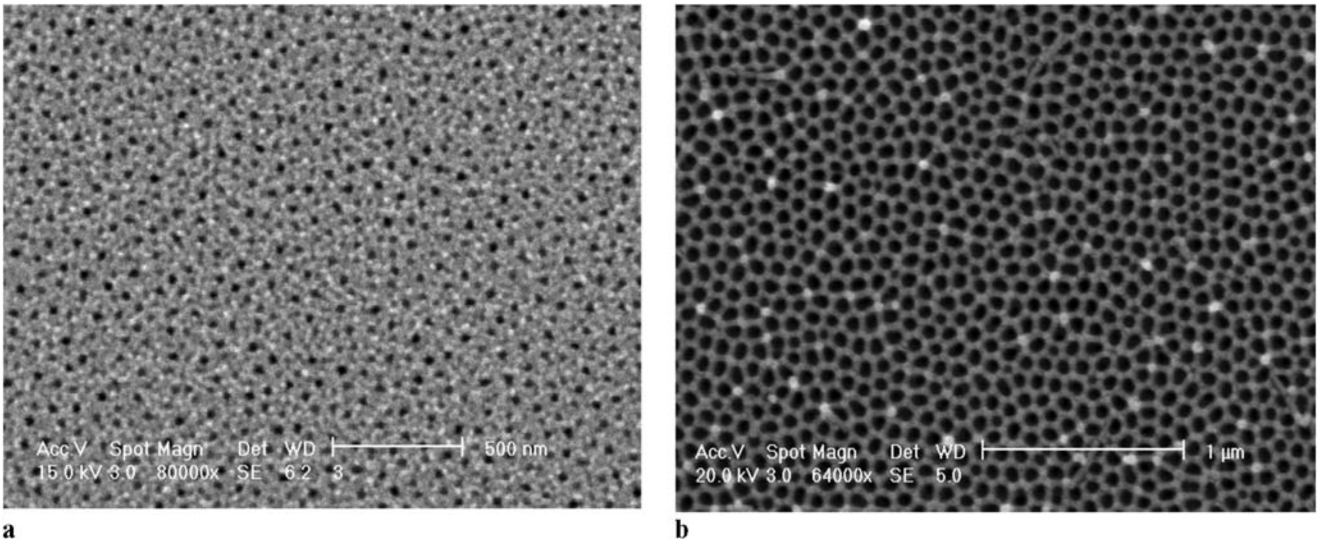

Fig. 4 SEM images of the AAO template/SiO_2/Si. **a** Top view of fabricated porous aluminum oxide film with nanopits after first anodization. **b** Top view of fabricated AAO template after second anodization

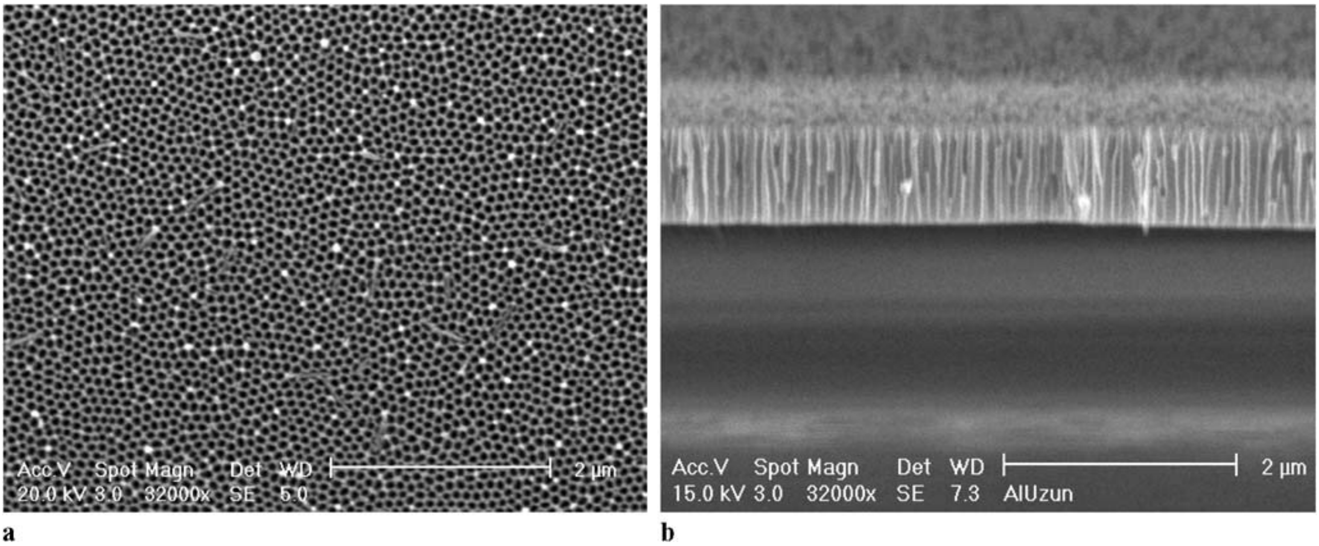

Fig. 5 SEM images of the AAO template/SiO_2/Si. **a** Top view of fabricated AAO template. **b** Cross-sectional view of fabricated AAO template

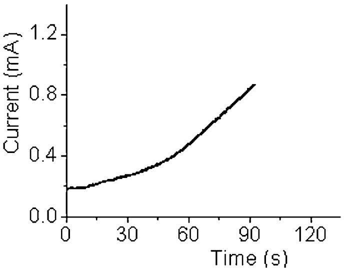

Fig. 6 Current–time transient during removing the alumina barrier layer of the AAO template/Ti/SiO_2/Si

Fig. 4a. The final pore arrangement has a high regularity after second anodization under the same conditions as the first shown in Figs. 4b and 5a.

In order to make electrical contacts to provide deposition of nanowires into the AAO template and to prevent the detachment of it, we used a titanium film with a thickness of 200 nm as a conducting and adhesion film between the aluminum film and the Si substrate. For opening up the blocked ends of the alumina barrier layer, we applied a negative potential to the AAO template in 0.2 M KCl solution. Figure 6 shows the current–time transient during removing the alumina barrier layer of the AAO template/Ti/SiO_2/Si.

After applying a negative voltage to the AAO template, the alumina barrier layer was charged negatively and positive ions (H^+, K^+) of electrolyte present in the template move to the layer. The H^+ take an electron on the surface of the alumina barrier layer and form H_2 gas that causes enrichment of electrolyte with KOH:

$$2H^+ + 2e^- \rightarrow \; H_2 \text{ (gas)}, \tag{4}$$

$$K^+ + OH^- \rightarrow \; KOH. \tag{5}$$

The formed KOH dissolves the alumina barrier layer according to the following reaction:

$$Al_2O_3 + 2KOH \rightarrow 2KAlO_2 + H_2O. \tag{6}$$

The titanium layer was oxidized while the Al film was anodizing, but a low-resistance titanium layer remained underneath this oxide layer. The current curve as a function of time was increased while KOH was beginning to open up the blocked ends of the alumina barrier layer; thus, AAO nanotubes were connected to titanium. We found that the alumina barrier layer must be removed in 100 s. Otherwise, if the current value rises to 0.8 mA, the ordered AAO nanotubes are broken and have some cracks on the top of the nanotubes due to the influence of the increasing pH value as the OH^- ions are increasing in the electrolyte. For this reason, we removed the alumina barrier layer until the current value increased to 0.8 mA. Figure 7 shows cross-sectional views of the AAO template/Ti/SiO_2/Si before and after removing the alumina barrier layer. An energy dispersive X-ray (EDX) spectrum from the surface of the AAO template/Ti/SiO2/Si after removing the alumina barrier layer confirms the process (Fig. 8).

The EDX spectra show Al signals from the alumina film, Ti signals from the titanium film, Si signals from the silicon substrate and O signals from the alumina film, the oxidized titanium film and the substrate. EDX spectra indicated that the interface between the Al_2O_3 and the Si substrate consists of Ti interconnected openings.

For removing the barrier layer, Rabin et al. [19] etched away the AAO film in a H_3PO_4:CrO_3 solution for 16 h. To adjust the pore diameter the alumina film was dipped in 5 wt.% H_3PO_4. Then, the barrier layer of the obtained 12-μm-thick AAO/Ti/SiO_2/Si structured AAO template was

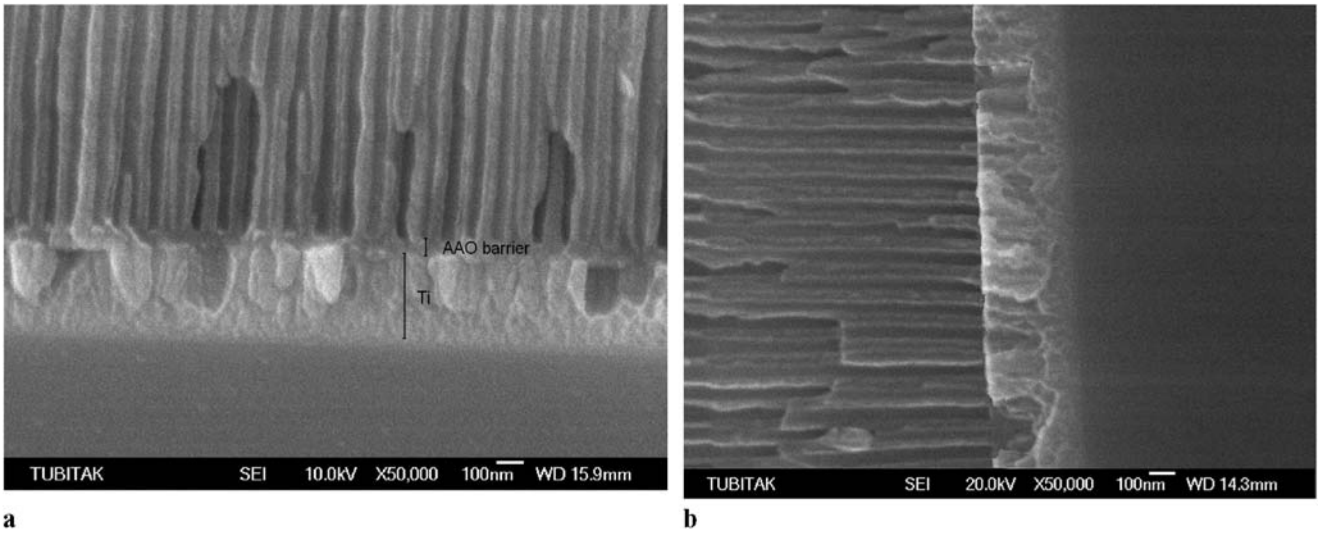

Fig. 7 Cross-sectional SEM images of the AAO template/Ti/SiO_2/Si. **a** Before removing the alumina barrier layer. **b** After removing the alumina barrier layer

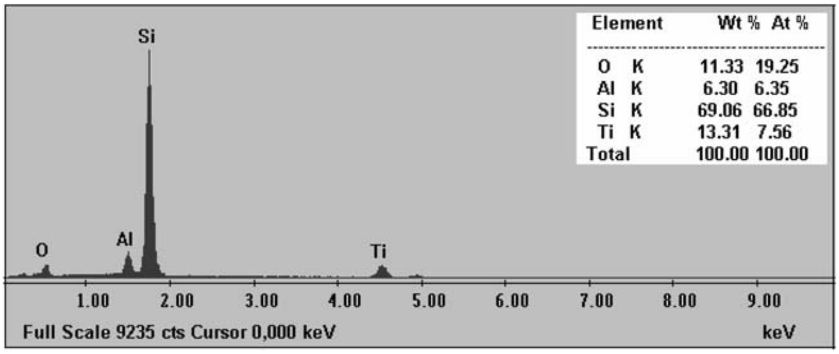

Element	Wt %	At %
O K	11.33	19.25
Al K	6.30	6.35
Si K	69.06	66.85
Ti K	13.31	7.56
Total	100.00	100.00

Fig. 8 EDX spectra from the surface of the AAO template/Ti/SiO_2/Si after removing the alumina barrier layer

removed by a cathodic polarization method in a dilute KCl solution. The barrier layer was electrochemically etched away by applying a cathodic bias of 2.25 V to the AAO template in a dilute KCl aqueous solution for 15–30 min. On the contrary, in this study, the AAO film was selectively chemical etched in 5 wt.% H_3PO_4 solution, which is commonly called a pore-widening solution for the AAO template. We used this solution as it has a significant advantage. This solution widened the nanotube size and thinned the AAO barrier layer at room temperature for only a few minutes, while the AAO film is selectively etching away, but it could not remove the barrier layer completely. Then, the thinned barrier layer was removed completely in KCl solution by cathodic polarization for a few seconds. Thus, AAO templates on Si were obtained with opened ends faster and more simply. Besides, the advantages of our study over the past studies are: (1) faster and more simple alumina etching and removing of the alumina barrier layer; (2) the AAO template/SiO_2/Si enables us to deposit vertical nanowires directly on Si substrates as nanowire-structured cathodes which can provide greater power density especially for fabrication of a chip-scale lithium (Li)-ion rechargeable microbattery; (3) the AAO template/Ti/SiO_2/Si enables us to deposit nanowires and nanotubes with an electrically conductive Ti film at the bottom especially for fabrication of chemical sensors and optoelectronic devices.

4 Summary

In summary, hexagonally well-ordered AAO template/SiO_2/Si and AAO template/Ti/SiO_2/Si were fabricated approximately 50 nm in diameter and 700 nm in length with 80-nm interpore distances. A novel process for removing the AAO barrier layer of both AAO template/SiO_2/Si and AAO template/Ti/SiO_2/Si was developed. We first widened the AAO nanotube size and thinned the AAO barrier layer at room temperature for only a few minutes and removed it completely in KCl solution by cathodic polarization for a few seconds. Thus, AAO templates on Si were obtained with opened ends faster and more simply. The process for the removal of the AAO barrier layer was given in detail in this paper.

Acknowledgements This study was supported by the Scientific and Technological Research Council of Turkey under project title 'Investigation and development of nanotechnologic hydrogen sensors' and Project No. 106T546.

References

1. S. Bandyopadhyay, H. Singh Nalwa (eds.), *Quantum Dots and Nanowires* (American Scientific, Stevenson Ranch, 2003)
2. I. Lombardi, A.I. Hochbaum, P.D. Yang, C. Carraro, R. Maboudian, Chem. Mater. **18**, 988 (2006)
3. M. Lahav, E.A. Weiss, Q.B. Xu, G.M. Whitesides, Nano Lett. **6**, 2166 (2006)
4. S. Zhao, H. Roberge, A. Yelon, T. Veres, J. Am. Chem. Soc. **128**, 12352 (2006)
5. H. Gao, N.N. Gosvami, J. Deng, L.-S. Tan, M.S. Sander, Langmuir **22**, 8087 (2006)
6. W. West, N. Myung, J. Whitacre, B. Ratnakumar, J. Power Sources **126**, 203 (2004)
7. H. Masuda, K. Fukuda, Science **268**, 1466 (1995)
8. O. Jessensky, F. Müller, U. Gösele, Appl. Phys. Lett. **72**, 1173 (1998)
9. V.P. Parkhutik, V.I. Shershulsky, J. Phys. D, Appl. Phys. **25**, 1258 (1992)
10. K. Nielsch, F. Müller, A.P. Li, U. Gösele, Adv. Mater. **12**, 582 (2000)
11. A.P. Li, F. Müller, A. Birner, K. Nielsch, U. Gösele, J. Appl. Phys. **84**, 6023 (1998)
12. O. Jessensky, F. Müller, U. Gösele, J. Electrochem. Soc. **145**, 3735 (1998)
13. W. Lee, R. Li, U. Gösele, K. Nielsch, Nat. Mater. **5**, 741 (2006)
14. X. Zhao, S.-K. Seo, U.-J. Lee, K.-H. Lee, J. Electrochem. Soc. **154**, C553 (2007)
15. R.C. Furneaux, W.R. Rigby, A.P. Davidson, Nature **337**, 147 (1989)
16. H.B. Xu, H.Z. Chen, W.J. Xu, M. Wang, Chem. Phys. Lett. **412**, 294 (2005)
17. S.K. Hwang, S.H. Jeong, O.J. Lee, K.H. Lee, Microelectron. Eng. **77**, 2 (2005)
18. A. Saedi, M. Ghorbani, Mater. Chem. Phys. **91**, 417 (2005)
19. O. Rabin, P.R. Herz, Y.M. Lin, A.I. Akinwande, B.S. Cronin, M.S. Dresselhaus, Adv. Funct. Mater. **13**, 8 (2003)
20. M. Tian, S. Xu, J. Wang, N. Kumar, E. Wertz, Q. Li, P.M. Campbell, M.H.W. Chan, T.E. Mallouk, Nano Lett. **5**, 4 (2005)
21. M.S. Sander, L.-S. Tan, Adv. Funct. Mater. **13**, 5 (2003)